Inertia-free fault-tolerant spacecraft attitude tracking using control allocation

Qiang Shen [a], Danwei Wang [a], Senqiang Zhu [a], Eng Kee Poh [a]

[a] *EXQUISITUS, Centre for E-City, Nanyang Technological University, 639798, Singapore*

Abstract

The problem of fault-tolerant attitude tracking control for an over-actuated spacecraft in the presence of actuator faults/failures and external disturbances is addressed in this paper. Assuming that information on the inertia and bounds on the disturbances are unknown, a novel fault-tolerant control (FTC) law incorporating on-line control allocation (CA) is developed to handle actuator faults/failures. To improve the robustness of the adaptive law and stop the adaptive gain from increasing, the time-varying dead-zone modification technique is employed in parameter adaptations. It is shown that uniform ultimate boundedness of the tracking errors can be ensured. To illustrate the efficiency of the CA-based FTC strategy, numerical simulations are carried out for a rigid spacecraft under actuator faults and failures.

Key words: Fault-tolerant control(FTC); Control allocation; Attitude tracking; Spacecraft control.

1 Introduction

Attitude tracking control of spacecraft systems is a benchmark control problem which is widely studied due to its highly coupled nonlinearity in dynamics [1]. Recently, various nonlinear control approaches, such as inverse optimal control [2], sliding mode control [3], [4], hybrid control [5], output feedback control [6], etc., have been proposed for solving the attitude tracking control problem with normal functioning actuators. However, in practical circumstances, actuators may experience complete failures or partial loss of effectiveness during operation [7], which could significantly degrade mission performance or even lead to totally loss of the spacecraft, see the example of satellite GPS BII-07 [8]. Therefore, to enhance the reliability of spacecraft, actuator fault tolerance capability needs to be developed in attitude control system design.

Fault-tolerant control (FTC) is one approach to ensure reliable operation of systems while maintaining desired stability and performance properties [9]. Generally, approaches for FTC systems design can be classified into two types, namely, passive and active ones [10]. The similarities and differences between these two FTC design methodologies from both philosophical and practical points of view can be found in [11]. Sliding mode control (SMC) technique has attracted extensive interest in FTC design recently due to its inherent robustness properties against matched uncertainties, see for example [12], [13], [14] and [15]. For spacecraft attitude control systems, methods such as multiple model [16], indirect robust adaptive control [17], dynamic inversion technique [18], and SMC [19], [20] etc., have been used to maintain the desired attitude maneuver in spite of actuator faults or failures.

Modern spacecraft often use redundant actuators to improve the reliability and survivability. To make effective use of these redundancies, control allocation (CA) is one promising and effective approach [21], which distributes the virtual control efforts from the high level controller to the individual actuators, especially in the case of actuator faults and failures [22], [23]. Recently, in [15], [24], [25], SMC technique is combined with CA to develop fault-tolerant controllers for over-actuated linear systems when actuators were subject to partial loss of effectiveness or complete failures. For some spacecraft missions, such as remote sensing or reconnaissance, the spacecraft is required to achieve rapid attitude maneuvering together with high targeting accuracy and stability between the maneuvers [26]. However, external disturbances were not taken into account in designing these CA-based FTC schemes. Moreover, due to fuel consumption, deployable appendage, sensor boom or articulation, the mass properties of the spacecraft may be uncertain or unknown, which makes the inertia matrix different from that determined during preflight testing [27], [28]. This inertia parameter discrepancy may lead to the degradation of attitude control performance [29].

⋆ Corresponding author D. Wang. Tel.: +65 6790 5376; fax: +65 6793 3318

Email addresses: qshen1@e.ntu.edu.sg (Qiang Shen), edwwang@ntu.edu.sg (Danwei Wang), sqzhu@ntu.edu.sg (Senqiang Zhu), eekpoh@ntu.edu.sg (Eng Kee Poh).

This paper aims to propose a novel inertia-free adaptive FTC design incorporated with CA for spacecraft attitude tracking systems in the presence of unknown physical inertia information, external disturbances, and actuator faults/failures. The main contributions of the paper are listed as follows: (1) the existing works that design CA-based FTC approach for linear systems in [15], [24], are extended to strongly coupled nonlinear attitude tracking systems, and external disturbances are rejected. (2) Some modifications are made for the on-line CA scheme proposed in [15] so that partially effective actuators can be leveraged for control use. (3) Unlike existing methods [2], [27] that estimate the elements in inertia matrix directly for solving the attitude tracking control problem, indirect adaptive techniques are employed so that inertia matrix information is not required in the FTC design. (4) Due to the structure of the proposed indirect adaptive control technique, a novel time-varying dead-zone modification is proposed in the design of parameter adaptations to stop the adaptive gain from increasing and improve robustness of the adaptive law to measurement or system noises.

The remaining of the paper is organized as follows. Section 2 presents the mathematic models for spacecraft attitude tracking systems with actuator fault/failure. Section 3 is devoted to the presentation of main contributions, where a novel CA-based inertia-free adaptive continuous FTC scheme is proposed. In Section 4, simulation results are included to show the efficiency of the proposed scheme. Finally, conclusions and future works are given in Section 5.

2 Problem Formulation

2.1 Spacecraft Attitude Dynamics

The kinematics and dynamics for the attitude motion of a rigid spacecraft is expressed as follows [30]:

$$\begin{cases} \dot{\boldsymbol{Q}} = \begin{bmatrix} \dot{\boldsymbol{q}} \\ \dot{q}_0 \end{bmatrix} = \frac{1}{2} \begin{bmatrix} \boldsymbol{S}(\boldsymbol{q}) + q_0 \boldsymbol{I}_3 \\ -\boldsymbol{q}^T \end{bmatrix} \boldsymbol{\omega} \\ \boldsymbol{J}\dot{\boldsymbol{\omega}} = -\boldsymbol{S}(\boldsymbol{\omega})\boldsymbol{J}\boldsymbol{\omega} + \boldsymbol{D}\boldsymbol{u} + \boldsymbol{d} \end{cases} \tag{1}$$

where $\boldsymbol{Q} = [q_1, q_2, q_3, q_0]^T = [\boldsymbol{q}^T, q_0]^T \in \mathbb{R}^3 \times \mathbb{R}$ denotes the unit-quaternion describing the attitude orientation of the body frame $\mathcal{B}$ with respect to inertial frame $\mathcal{I}$ and satisfies the constraint $\boldsymbol{q}^T\boldsymbol{q} + q_0^2 = 1$, $\boldsymbol{\omega} \in \mathbb{R}^3$ is the inertial angular velocity vector of the spacecraft with respect to an inertial frame $\mathcal{I}$ and expressed in the body frame $\mathcal{B}$, $\boldsymbol{J} \in \mathbb{R}^{3\times3}$ denotes inertia matrix of the spacecraft, $\boldsymbol{I}_3 \in \mathbb{R}^{3\times3}$ denotes a 3-by-3 identity matrix, $\boldsymbol{D} \in \mathbb{R}^{3\times N}$ (N is the number of actuators and $N > 3$) is the actuator distribution matrix with full row rank, i.e., $\text{rank}(\boldsymbol{D}) = 3$, $\boldsymbol{u} \in \mathbb{R}^N$ and $\boldsymbol{d} \in \mathbb{R}^3$ denote the control torques produced by the N actuators and external disturbances, respectively. The matrix $\boldsymbol{S}(\boldsymbol{x}) \in \mathbb{R}^{3\times3}$ is a skew-symmetric matrix satisfying $\boldsymbol{S}(\boldsymbol{x})\boldsymbol{y} = \boldsymbol{x}\times\boldsymbol{y}$ for any vectors $\boldsymbol{x}, \boldsymbol{y} \in \mathbb{R}^3$, and $\times$ denotes vector cross product.

In the fault-free situation, the actual output torques $\boldsymbol{u}$ of N actuators are equal to the desired values $\boldsymbol{u}_c = [u_{c1}, u_{c2}, \ldots, u_{cN}]^T \in \mathbb{R}^N$ commanded by the controller, i.e., $\boldsymbol{u} = \boldsymbol{u}_c$. When the system experiences actuator faults/failures, the nonlinear attitude dynamics can be rewritten in the following form:

$$\boldsymbol{J}\dot{\boldsymbol{\omega}} = -\boldsymbol{S}(\boldsymbol{\omega})\boldsymbol{J}\boldsymbol{\omega} + \boldsymbol{D}\boldsymbol{E}(t)\boldsymbol{u}_c + \boldsymbol{d} \tag{2}$$

where $\boldsymbol{E} = \text{diag}\{e_1(t), e_2(t), \ldots, e_N(t)\} \in \mathbb{R}^{N\times N}$ is the effectiveness gain matrix of actuators with scalars $e_i(t)$ satisfying $0 \le e_i \le 1$, $i = 1, 2, \ldots, N$. Note that the case $e_i(t) = 1$ indicates that the ith actuator works normally, and $0 < e_i(t) < 1$ implies that the ith actuator partially loses its effectiveness. The value $e_i(t) = 0$ means that the ith actuator undergoes a complete failure. In this paper, it is assumed that the actuator effectiveness gain can be diagnosed by an FDD mechanism. Similar to [15], the estimate of the actuator effectiveness, $\widehat{\boldsymbol{E}}(t) = diag\{\hat{e}_1(t), \hat{e}_2(t), \ldots, \hat{e}_N(t)\}$ with $0 \le \hat{e}_i(t) \le 1$, are supposed to satisfy

$$\boldsymbol{E}(t) = (\boldsymbol{I}_N - \boldsymbol{\Delta}(t))\widehat{\boldsymbol{E}}(t) \tag{3}$$

where $\boldsymbol{\Delta}(t) = diag\{\delta_1(t), \delta_2(t), \ldots, \delta_N(t)\}$, and the unknown scalars $\delta_i(t)$ represent the level of imprecision in the estimation of actuator effectiveness. Since the values of $\boldsymbol{E}$ and $\widehat{\boldsymbol{E}}$ are constrained between zero and one, the mismatch $\boldsymbol{\Delta}(t)$ would be bounded by a constant Δ_{max}, i.e., $\|\boldsymbol{\Delta}(t)\| \le \Delta_{max}$, where the notation $\|\cdot\|$ denotes the Euclidean norm or its induced norm.

2.2 Attitude Error Dynamics

To address the attitude tracking issue, the desired motion of the spacecraft is given in a desired reference frame $\mathcal{R}$, whose orientation with respect to $\mathcal{I}$ is specified by unit-quaternion $\boldsymbol{Q}_d = [\boldsymbol{q}_d^T, q_{d0}]^T$ and satisfies the constraint $\boldsymbol{q}_d^2 + q_{d0}^2 = 1$. The attitude tracking error $\boldsymbol{Q}_e = [\boldsymbol{q}_e^T, q_{e0}]^T = \boldsymbol{Q}_d^{-1} \otimes \boldsymbol{Q}$ is defined as the relative orientation between the attitude $\boldsymbol{Q}$ and the desired attitude $\boldsymbol{Q}_d$, where $\boldsymbol{Q}_d^{-1}$ is the conjugate of the desired quaternion determined by $\boldsymbol{Q}_d^{-1} = [-\boldsymbol{q}_d^T, q_{d0}]^T$, and $\otimes$ denotes the quaternion multiplication operator. The angular velocity error $\boldsymbol{\omega}_e \in \mathbb{R}^3$ is given by $\boldsymbol{\omega}_e = \boldsymbol{\omega} - \boldsymbol{R}(\boldsymbol{Q}_e)\boldsymbol{\omega}_d$, where $\boldsymbol{\omega}_d$ is the desired angular velocity expressed in the desired reference frame $\mathcal{R}$. The rotation matrix $\boldsymbol{R}(\boldsymbol{Q}_e)$ is given by $\boldsymbol{R}(\boldsymbol{Q}_e) = (q_{e0}^2 - \boldsymbol{q}_e^T\boldsymbol{q}_e)\boldsymbol{I_3} + 2\boldsymbol{q}_e\boldsymbol{q}_e^T - 2q_{e0}\boldsymbol{S}(\boldsymbol{q}_e)$, and $\|\boldsymbol{R}(\boldsymbol{Q}_e)\| = 1$ and $\dot{\boldsymbol{R}}(\boldsymbol{Q}_e) = -\boldsymbol{S}(\boldsymbol{\omega}_e)\boldsymbol{R}(\boldsymbol{Q}_e)$.

Thus, the equation that governs the attitude tracking error in terms of the unit-quaternion is given by

$$\dot{\boldsymbol{Q}}_e = \begin{bmatrix} \dot{\boldsymbol{q}}_e \\ \dot{q}_{e0} \end{bmatrix} = \frac{1}{2} \begin{bmatrix} \boldsymbol{S}(\boldsymbol{q}_e) + q_{e0}\boldsymbol{I}_3 \\ -\boldsymbol{q}_e^T \end{bmatrix} \boldsymbol{\omega}_e \,. \tag{4}$$

To develop the control scheme, it would be useful to define an auxiliary desired angular velocity, given by

$$\bar{\boldsymbol{\omega}}_d = \boldsymbol{R}(\boldsymbol{Q}_e)\boldsymbol{\omega}_d - k\boldsymbol{q}_e, \tag{5}$$

where k is a positive constant chosen by the designer. The differentiable signal $\bar{\boldsymbol{\omega}}_d$ satisfies

$$\begin{aligned}\dot{\bar{\boldsymbol{\omega}}}_d =& -\boldsymbol{S}(\boldsymbol{\omega}_e)\boldsymbol{R}(\boldsymbol{Q}_e)\boldsymbol{\omega}_d + \boldsymbol{R}(\boldsymbol{Q}_e)\dot{\boldsymbol{\omega}}_d \\ & -\frac{k}{2}\left(\boldsymbol{S}(\boldsymbol{q}_e)+q_{e0}\boldsymbol{I}_3\right)\boldsymbol{\omega}_e. \end{aligned} \tag{6}$$

Based on the auxiliary desired angular velocity, a sliding vector is given by [31], [32]

$$\tilde{\boldsymbol{\omega}} = \boldsymbol{\omega} - \bar{\boldsymbol{\omega}}_d = \boldsymbol{\omega}_e + k\boldsymbol{q}_e. \tag{7}$$

Consequently, from the attitude dynamics in (2) with actuator efficiency in (3), the attitude tracking error in terms of the sliding vector can be described as

$$\begin{aligned}\boldsymbol{J}\dot{\tilde{\boldsymbol{\omega}}} =& -\boldsymbol{S}(\tilde{\boldsymbol{\omega}})\boldsymbol{J}\boldsymbol{\omega} - \boldsymbol{S}(\bar{\boldsymbol{\omega}}_d)\boldsymbol{J}\boldsymbol{\omega} - \boldsymbol{J}\dot{\bar{\boldsymbol{\omega}}}_d \\ & + \boldsymbol{D}(\boldsymbol{I}_N - \boldsymbol{\Delta}(t))\widehat{\boldsymbol{E}}(t)\boldsymbol{u}_c + \boldsymbol{d}. \end{aligned} \tag{8}$$

To facilitate control system design, the following assumptions are used in the subsequent developments.

Assumption 1 *The inertia matrix $\boldsymbol{J}$ is a symmetric, positive-definite and unknown constant matrix such that $\|\boldsymbol{J}\| \le c_J$, where c_J is a positive constant.*

Assumption 2 *The desired angular velocity of spacecraft and its time derivative are bounded, that is $\|\boldsymbol{\omega}_d\| \le c_\omega$ and $\|\dot{\boldsymbol{\omega}}_d\| \le c_{d\omega}$, where c_ω and $c_{d\omega}$ are positive constants.*

Assumption 3 *The external disturbance $\boldsymbol{d}$ is bounded such that $\|\boldsymbol{d}\| \le d_{max}$, where d_{max} is a positive constant.*

Assumption 4 *The spacecraft is so constructed that potentially up to $N-3$ actuators can suffer from total failures simultaneously, and the estimate of the actuator effectiveness satisfies $\widehat{\boldsymbol{E}}(t) \in \mathcal{E}$, where set $\mathcal{E}$ is defined as*

$$\mathcal{E} = \left\{(\hat{e}_1, \hat{e}_2, \ldots, \hat{e}_N) \in [0\ 1]^N : det(\boldsymbol{D}\widehat{\boldsymbol{E}}^3(t)\boldsymbol{D}^T) \neq 0\right\}$$

$$with\ [0\ 1]^N = \underbrace{[0\ 1] \times \cdots \times [0\ 1]}_{N\ times}.$$

Remark 1. Since the environmental disturbances due to gravitation, solar radiation pressure, magnetic forces or aerodynamic drag are bounded in practice, assumption 3 is reasonable. Assumption 4 guarantees that the faulty attitude tracking system is controllable and closed-loop stability can be maintained, otherwise the attitude tracking system shall be under-actuated.

2.3 Problem Formulation

In this paper, actuator redundancy ($N > 3$) is considered to enhance reliability and safety for the attitude tracking control system, and hence the attitude tracking control system is an over-actuated systems. Thus, it is possible to divide the controller design into two parts

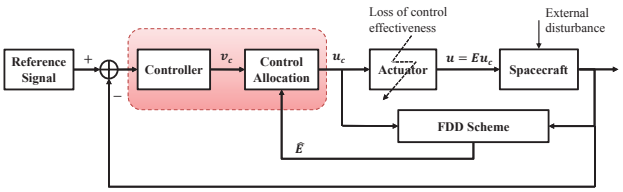

Fig. 1. Structure of the overall attitude tracking scheme.

[21]: high level controller design and CA design. A high level controller is designed as virtual control input to specify total desired control efforts to the system, while CA is developed to map the virtual control efforts into individual actuators such that the total actual control signals generated by all actuators amount to commanded virtual inputs. Overall structure of the CA-based fault-tolerant attitude tracking scheme is shown in Fig. 1.

Motivated by [15], the following l_2-optimal CA problem is considered:

$$\begin{aligned}\min_{\boldsymbol{u}_c(t)} \quad & \boldsymbol{u}_c^T\widehat{\boldsymbol{E}}^{-1}(t)\boldsymbol{u}_c \\ \text{subject to} \quad & \boldsymbol{D}\widehat{\boldsymbol{E}}(t)\boldsymbol{u}_c = \boldsymbol{v}_c \end{aligned} \tag{9}$$

where $\boldsymbol{v}_c$ is the virtual control input generated by the high level controller. It should be noted that $\boldsymbol{D}\widehat{\boldsymbol{E}}^3(t)\boldsymbol{D}^T$ is invertible since $\widehat{\boldsymbol{E}}(t) \in \mathcal{E}$ from assumption 4. Comparing with the existing CA scheme in [15], the difference is that the estimate of the actuator effectiveness is considered in the constraint. This modification makes the constraint is in accord with the actual situation, and partially effective actuators can be leveraged for control use. Then, it is straightforward to get the solution of (9) as

$$\boldsymbol{u}_c = \widehat{\boldsymbol{E}}^2(t)\boldsymbol{D}^T(\boldsymbol{D}\widehat{\boldsymbol{E}}^3(t)\boldsymbol{D}^T)^{-1}\boldsymbol{v}_c. \tag{10}$$

Substituting the CA solution (10) into (8), the attitude tracking error dynamics can be further written as

$$\begin{aligned}\boldsymbol{J}\dot{\tilde{\boldsymbol{\omega}}} =& -\boldsymbol{S}(\tilde{\boldsymbol{\omega}})\boldsymbol{J}\boldsymbol{\omega} - \boldsymbol{S}(\bar{\boldsymbol{\omega}}_d)\boldsymbol{J}\boldsymbol{\omega} - \boldsymbol{J}\dot{\bar{\boldsymbol{\omega}}}_d + \boldsymbol{v}_c \\ & - \boldsymbol{D}\boldsymbol{\Delta}(t)\boldsymbol{D}^\dagger\boldsymbol{v}_c + \boldsymbol{d}, \end{aligned} \tag{11}$$

where $\boldsymbol{D}^\dagger = \widehat{\boldsymbol{E}}^3(t)\boldsymbol{D}^T(\boldsymbol{D}\widehat{\boldsymbol{E}}^3(t)\boldsymbol{D}^T)^{-1}$. Since $\boldsymbol{D}\boldsymbol{D}^\dagger = \boldsymbol{I}_3$, $\boldsymbol{D}^\dagger$ is a pseudo-inverse of matrix $\boldsymbol{D}$ under the condition that $\widehat{\boldsymbol{E}}(t) \in \mathcal{E}$ in assumption 4. According to the property of pseudo-inverse in [33], if $\widehat{\boldsymbol{E}}(t) \in \mathcal{E}$, then there exists a finite scalar ξ independent of $\widehat{\boldsymbol{E}}(t)$ such that

$$\|\boldsymbol{D}^\dagger\| = \|\widehat{\boldsymbol{E}}^3(t)\boldsymbol{D}^T(\boldsymbol{D}\widehat{\boldsymbol{E}}^3(t)\boldsymbol{D}^T)^{-1}\| < \xi. \tag{12}$$

Assumption 5 *The maximal mismatch between the actual efficiency matrix $\boldsymbol{E}(t)$ and its estimate $\widehat{\boldsymbol{E}}(t)$ in (3) satisfies $\Delta_{max}\xi\|\boldsymbol{D}\| < 1$, where ξ is defined in (12).*

Remark 2. Assumption 5 means that the mismatch between the actual efficiency matrix $\boldsymbol{E}(t)$ and its estimate $\widehat{\boldsymbol{E}}(t)$ cannot be arbitrarily large. In practice, since the designed FDD scheme could always provide estimation on faults with a certain degree of precision, this assumption is reasonable.

3 Inertia-free Adaptive FTC Design

In this section, an inertia-free adaptive continuous virtual control input is proposed to achieve attitude tracking under actuator faults/failures without requiring spacecraft inertia knowledge. To eliminate the requirement of inertia information, indirect adaptive technique is employed. First, using assumptions 1-3 and properties that $\|\boldsymbol{R}(\boldsymbol{Q}_e)\| = 1$ and $\|\boldsymbol{S}(\boldsymbol{q}_e) + q_{e0}\boldsymbol{I}_3\| = 1$, the following inequalities are established:

$$\|\bar{\boldsymbol{\omega}}_d\| \leq c_\omega + k, \tag{13}$$
$$\|\boldsymbol{S}(\bar{\boldsymbol{\omega}}_d)\boldsymbol{J}\boldsymbol{\omega}\| \leq c_J\,(c_\omega + k)\,\|\boldsymbol{\omega}\|, \tag{14}$$
$$\|\dot{\bar{\boldsymbol{\omega}}}_d\| \leq \left(c_\omega + \frac{k}{2}\right)\|\boldsymbol{\omega}\| + c_\omega^2 + \frac{k}{2}c_\omega + c_{d\omega}. \tag{15}$$

Consequently, the lumped nonlinear terms and external disturbances in (8) are upper bounded by

$$\|\boldsymbol{S}(\bar{\boldsymbol{\omega}}_d)\boldsymbol{J}\boldsymbol{\omega} + \boldsymbol{J}\dot{\bar{\boldsymbol{\omega}}}_d + \boldsymbol{d}\| \leq c\Theta \tag{16}$$

where the unknown constant c is given by

$$c = \max\left\{c_J\Big(2c_\omega + \frac{3}{2}k\Big), c_J\Big(c_\omega^2 + \frac{k}{2}c_\omega + c_{d\omega}\Big) + d_{max}\right\}$$

and the time-varying variable Θ is defined as

$$\Theta = \|\boldsymbol{\omega}\| + 1. \tag{17}$$

Next, the inertia-free adaptive continuous virtual control input for the spacecraft is proposed as

$$\boldsymbol{v}_c = \boldsymbol{v}_1 + \boldsymbol{v}_2 \tag{18}$$
$$\boldsymbol{v}_1 = -k_1\tilde{\boldsymbol{\omega}} - k_2\boldsymbol{q}_e \tag{19}$$
$$\boldsymbol{v}_2 = -\frac{k_v + \hat{c}(t)\Theta + \Delta_{max}\xi\|\boldsymbol{D}\|\|\boldsymbol{v}_1\|}{1 - \Delta_{max}\xi\|\boldsymbol{D}\|}\tilde{\boldsymbol{\omega}}_a \tag{20}$$
$$\tilde{\boldsymbol{\omega}}_a = \begin{cases} \frac{\tilde{\boldsymbol{\omega}}}{\|\tilde{\boldsymbol{\omega}}\|}, & \text{if } \|\tilde{\boldsymbol{\omega}}\| > \epsilon \\ \frac{\tilde{\boldsymbol{\omega}}}{\epsilon}, & \text{if } \|\tilde{\boldsymbol{\omega}}\| \leq \epsilon \end{cases} \tag{21}$$

where k_1 and k_2 are two positive constants, ϵ is a positive scalar variable defined as $\epsilon = \frac{\sigma}{\Theta}$, and σ is a small positive constant. Since $\Theta = \|\boldsymbol{\omega}\| + 1 \geq 1$, it is clear that $\epsilon \leq \sigma$. The parameter $\hat{c}(t)$ is the estimate of constant c, which is updated as

$$\dot{\hat{c}}(t) = \alpha_1\Theta\tilde{\boldsymbol{\omega}}_a^T\boldsymbol{D}_\epsilon[\tilde{\boldsymbol{\omega}}] - \frac{\alpha_1\alpha_2}{\Theta}\hat{c}(t) \tag{22}$$

where α_1 and α_2 are two positive constants, and $\hat{c}(0) > 0$. The dead-zone operator $\boldsymbol{D}_\epsilon[\cdot]$ is defined as

$$\boldsymbol{D}_\epsilon[\tilde{\boldsymbol{\omega}}] = \begin{cases} \tilde{\boldsymbol{\omega}}, & \text{if } \|\tilde{\boldsymbol{\omega}}\| > \epsilon \\ \boldsymbol{0}, & \text{if } \|\tilde{\boldsymbol{\omega}}\| \leq \epsilon. \end{cases} \tag{23}$$

Since the time-varying variable Θ is incorporated into ϵ, the dead-zone width ϵ is also time-varying. The properties of $\tilde{\boldsymbol{\omega}}_a$ and Θ are described by the following lemmas.

Lemma 1 *The function $\tilde{\boldsymbol{\omega}}_a$ defined in* (21) *has the following properties:*

(1) $\|\tilde{\boldsymbol{\omega}}_a\| \leq 1$.
(2) $\tilde{\boldsymbol{\omega}}^T\tilde{\boldsymbol{\omega}}_a = \|\tilde{\boldsymbol{\omega}}\|$, *if* $\|\tilde{\boldsymbol{\omega}}\| > \epsilon$
$\tilde{\boldsymbol{\omega}}^T\tilde{\boldsymbol{\omega}}_a \leq \sigma$, *if* $\|\tilde{\boldsymbol{\omega}}\| \leq \epsilon$.

Proof. See the appendix A. □

Lemma 2 *For $\|\tilde{\boldsymbol{\omega}}\| \leq \epsilon$, the variable Θ defined in* (17) *is bounded by*

$$1 \leq \Theta \leq \Theta_m \tag{24}$$

where the finite constant $\Theta_m = \frac{c_\omega + k + 1 + \sqrt{(c_\omega + k + 1)^2 + 4\sigma}}{2}$.

Proof. See the appendix B. □

To analyze the stability of the overall system, a Lyapunov-like candidate V_s is proposed as

$$V_s = \frac{1}{2}\tilde{\boldsymbol{\omega}}^T\boldsymbol{J}\tilde{\boldsymbol{\omega}} + k_2\left[\boldsymbol{q}_e^T\boldsymbol{q}_e + (1 - q_{e0})^2\right] + \frac{1}{2\alpha_1}\tilde{c}^2(t) \tag{25}$$

where $\tilde{c}(t) = c - \hat{c}(t)$, and $\dot{\tilde{c}}(t) = -\dot{\hat{c}}(t)$. The time derivative of V_s is given by

$$\begin{aligned}\dot{V}_s = \tilde{\boldsymbol{\omega}}^T\Big(&- \boldsymbol{S}(\tilde{\boldsymbol{\omega}})\boldsymbol{J}\boldsymbol{\omega} - \boldsymbol{S}(\bar{\boldsymbol{\omega}}_d)\boldsymbol{J}\boldsymbol{\omega} - \boldsymbol{J}\dot{\bar{\boldsymbol{\omega}}}_d + \boldsymbol{d} \\ &- \boldsymbol{D}\boldsymbol{\Delta}(t)\widehat{\boldsymbol{E}}^3(t)\boldsymbol{D}^T(\boldsymbol{D}\widehat{\boldsymbol{E}}^3(t)\boldsymbol{D}^T)^{-1}\boldsymbol{v}_c + \boldsymbol{v}_c\Big) \\ &+ k_2\boldsymbol{q}_e^T\boldsymbol{\omega}_e - \frac{1}{\alpha_1}\tilde{c}(t)\dot{\hat{c}}(t).\end{aligned} \tag{26}$$

Since $\hat{c}(0) > 0$ is chosen, $\hat{c}(t) \geq 0$ can always be guaranteed in view of the update law of $\hat{c}(t)$ in (22). Consequently, under assumption 5 and using the first property in lemma 1, it follows that $\|\boldsymbol{v}_c\| \leq \frac{k_v + \hat{c}(t)\Theta + \|\boldsymbol{v}_1\|}{1 - \Delta_{max}\xi\|\boldsymbol{D}\|}$. Substituting the inertia-free virtual control input (18) and parameter update law (22) into (26), it leads to

$$\begin{aligned}\dot{V}_s \leq\ &-k_1\|\tilde{\boldsymbol{\omega}}\|^2 - k_2k\|\boldsymbol{q}_e\|^2 + c\Theta\|\tilde{\boldsymbol{\omega}}\| \\ &+\Delta_{max}\xi\|\boldsymbol{D}\|\frac{k_v + \hat{c}(t)\Theta + \|\boldsymbol{v}_1\|}{1 - \Delta_{max}\xi\|\boldsymbol{D}\|}\|\tilde{\boldsymbol{\omega}}\| \\ &-\frac{k_v + \hat{c}(t)\Theta + \Delta_{max}\xi\|\boldsymbol{D}\|\|\boldsymbol{v}_1\|}{1 - \Delta_{max}\xi\|\boldsymbol{D}\|}\tilde{\boldsymbol{\omega}}^T\tilde{\boldsymbol{\omega}}_a \\ &-\tilde{c}(t)\Theta\tilde{\boldsymbol{\omega}}_a^T\boldsymbol{D}_\epsilon[\tilde{\boldsymbol{\omega}}] + \frac{\alpha_2}{\Theta}\tilde{c}(t)\hat{c}(t).\end{aligned} \tag{27}$$

For further stability analysis, two cases are considered.

Case I: If $\|\tilde{\boldsymbol{\omega}}\| > \epsilon$, then $\tilde{\boldsymbol{\omega}}^T\tilde{\boldsymbol{\omega}}_a = \|\tilde{\boldsymbol{\omega}}\|$ and $\boldsymbol{D}_\epsilon[\tilde{\boldsymbol{\omega}}] = \tilde{\boldsymbol{\omega}}$. Therefore, (27) can be rewritten as

$$\begin{aligned}\dot{V}_s \leq\ &-k_1\|\tilde{\boldsymbol{\omega}}\|^2 - k_2k\|\boldsymbol{q}_e\|^2 - \tilde{c}(t)\Theta\|\tilde{\boldsymbol{\omega}}\| \\ &+\frac{\alpha_2}{\Theta}\tilde{c}(t)\hat{c}(t) + \frac{k_v\Delta_{max}\xi\|\boldsymbol{D}\| - k_v}{1 - \Delta_{max}\xi\|\boldsymbol{D}\|}\|\tilde{\boldsymbol{\omega}}\| \\ &+\frac{\hat{c}\Theta\Delta_{max}\xi\|\boldsymbol{D}\| + \tilde{c}(t)\Theta - c\Theta\Delta_{max}\xi\|\boldsymbol{D}\|}{1 - \Delta_{max}\xi\|\boldsymbol{D}\|}\|\tilde{\boldsymbol{\omega}}\| \\ \leq\ &-k_1\|\tilde{\boldsymbol{\omega}}\|^2 - k_2k\|\boldsymbol{q}_e\|^2 - k_v\|\tilde{\boldsymbol{\omega}}\| + \frac{\alpha_2}{\Theta}\tilde{c}(t)\hat{c}(t).\end{aligned} \tag{28}$$

By completion of squares that $\tilde{c}(t)\hat{c}(t) \leq -\frac{\tilde{c}^2(t)}{2} + \frac{c^2}{2}$ and using $\|\tilde{\boldsymbol{\omega}}\| > \frac{\sigma}{\Theta}$, it can be shown that

$$\dot{V}_s \leq -k_1\|\tilde{\boldsymbol{\omega}}\|^2 - k_2 k\|\boldsymbol{q}_e\|^2 - \frac{1}{\Theta}\left(k_v\sigma - \frac{\alpha_2 c^2}{2}\right). \quad (29)$$

If the design parameters k_v, σ, and α_2 are chosen so that

$$k_v\sigma \geq \frac{\alpha_2 c^2}{2}, \quad (30)$$

then $\dot{V}_s \leq -k_1\|\tilde{\boldsymbol{\omega}}\|^2 - k_2 k\|\boldsymbol{q}_e\|^2 < 0$. Therefore, when $\|\tilde{\boldsymbol{\omega}}\| > \epsilon$, $V_s(t)$ decreases monotonically until $\|\tilde{\boldsymbol{\omega}}\| \leq \epsilon$ is achieved. Consequently, $V_s(t)$ is upper bounded by its initial value $V_s(0)$, i.e., $V_s(t) \leq V_s(0)$. Since $\tilde{c}^2(t) \leq 2\alpha_1 V_s(t)$ from (25), it follows that

$$\hat{c}(t) \leq c_m \quad (31)$$

where $c_m = c + \sqrt{2\alpha_1 V_s(0)}$.

Case II: If $\|\tilde{\boldsymbol{\omega}}\| \leq \epsilon$, then $\tilde{\boldsymbol{\omega}}^T\tilde{\boldsymbol{\omega}}_a = \frac{\|\tilde{\boldsymbol{\omega}}\|^2}{\epsilon} \leq \sigma$ from the second property in lemma 1 and $\boldsymbol{D}_\epsilon[\tilde{\boldsymbol{\omega}}] = \boldsymbol{0}$. Therefore, (27) can be rewritten as

$$\begin{aligned}\dot{V}_s \leq\ & -k_1\|\tilde{\boldsymbol{\omega}}\|^2 - k_2 k\|\boldsymbol{q}_e\|^2 - \frac{\alpha_2}{2\Theta_m}\tilde{c}^2(t) + \frac{\alpha_2 c^2}{2} + c\Theta\|\tilde{\boldsymbol{\omega}}\| \\ & + \frac{\Delta_{max}\xi\|D\|}{1-\Delta_{max}\xi\|D\|}\left(k_v + \hat{c}\Theta + \|\boldsymbol{v}_1\|\right)\|\tilde{\boldsymbol{\omega}}\|. \quad (32)\end{aligned}$$

Assuming that $\|\tilde{\boldsymbol{\omega}}\| \leq \epsilon$ is satisfied at $t = t^*$. As soon as $\|\tilde{\boldsymbol{\omega}}\| \leq \epsilon$ is fulfilled at $t = t^*$, the adaptive parameter $\hat{c}(t)$ deceases monotonically in accordance with $\dot{\hat{c}}(t) = -\frac{\alpha_1\alpha_2}{\Theta}\hat{c}(t)$, which implies $\hat{c}(t) \leq \hat{c}(t^*)$. If $t^* = 0$ or $\|\tilde{\boldsymbol{\omega}}\|$ increase to ϵ at $t = t^*$, then $\hat{c}(t^*) \leq \hat{c}(0)$. Otherwise, $\|\tilde{\boldsymbol{\omega}}\|$ decreases to ϵ at $t = t^*$, and it follows from (31) that $\hat{c}(t^*) \leq c_m$. Since $\hat{c}(0) \leq V_s(0)$, it can always be guaranteed that $\hat{c}(t) \leq c_m$. Therefore, from (32) and using the constraint of unit-quaternion $|q_0| \leq 1$ as well as $\Theta\|\tilde{\boldsymbol{\omega}}\| \leq \sigma$ when $\|\tilde{\boldsymbol{\omega}}\| \leq \epsilon$, it is clear that

$$\begin{aligned}\dot{V}_s \leq\ & -k_1\|\tilde{\boldsymbol{\omega}}\|^2 - k_2 k\|\boldsymbol{q}_e\|^2 - \frac{\alpha_2}{2\Theta_m}\tilde{c}^2(t) + \frac{\alpha_2 c^2}{2} + c\sigma \\ & + \frac{\Delta_{max}\xi\|D\|}{1-\Delta_{max}\xi\|D\|}\left(k_v + c_m + k_2 + k_1\sigma\right)\sigma \quad (33)\end{aligned}$$

which leads to

$$\dot{V}_s \leq -\kappa V_s + \varrho \quad (34)$$

where the two positive constants κ and ϱ are given by $\kappa = \min\left\{\frac{k_1}{c_J}, k, \frac{\alpha_1\alpha_2}{\Theta_m}\right\}$ and $\varrho = \frac{\Delta_{max}\xi\|D\|}{1-\Delta_{max}\xi\|D\|}(k_v + c_m + k_2 + k_1\sigma)\sigma + \frac{\alpha_2 c^2}{2} + c\sigma + 4k_2 k$. In addition, let η be a constant defined as

$$\begin{aligned}\eta =\ & \frac{\Delta_{max}\xi\|D\|}{1-\Delta_{max}\xi\|D\|}\left(k_v + c_m + k_2 + k_1\sigma\right)\sigma \\ & + \frac{\alpha_2 c^2}{2} + c\sigma. \quad (35)\end{aligned}$$

Then, according to (33), it can be found that $\dot{V}_s(t) < 0$ if

$$\|\tilde{\boldsymbol{\omega}}\| > \sqrt{\frac{\eta}{k_1}}, \ \texttt{or}\ \|\boldsymbol{q}_e\| > \sqrt{\frac{\eta}{k_2 k}}. \quad (36)$$

Moreover, to show that angular velocity tracking error $\boldsymbol{\omega}_e$ is bounded as well, a new Lyapunov-like candidate is chosen as

$$\begin{aligned}V_{s1} =\ & \frac{1}{2}\tilde{\boldsymbol{\omega}}^T\boldsymbol{J}\tilde{\boldsymbol{\omega}} + (2k_1 k + k_2)\left[\boldsymbol{q}_e^T\boldsymbol{q}_e + (1-q_{e0})^2\right] \\ & + \frac{1}{2\alpha_1}\tilde{c}^2(t). \quad (37)\end{aligned}$$

Following the same lines as in the proof of *Case II* and using (7), it is straightforward to show that

$$\dot{V}_{s1} \leq -k_1\|\boldsymbol{\omega}_e\|^2 - k(k_1 k + k_2)\|\boldsymbol{q}_e\|^2 + \eta. \quad (38)$$

Clearly, according to (38), $\dot{V}_{s1}(t) < 0$ if

$$\|\boldsymbol{\omega}_e\| > \sqrt{\frac{\eta}{k_1}}, \ \texttt{or}\ \|\boldsymbol{q}_e\| > \sqrt{\frac{\eta}{k(k_1 k + k_2)}}. \quad (39)$$

Finally, the actual inertia-free adaptive continuous commanded control input, which will be sent to the actuator, is given by

$$\begin{aligned}\boldsymbol{u}_c =\ & \widehat{\boldsymbol{E}}^2(t)\boldsymbol{D}^T(\boldsymbol{D}\widehat{\boldsymbol{E}}^3(t)\boldsymbol{D}^T)^{-1}\Bigg(-k_1\tilde{\boldsymbol{\omega}} - k_2\boldsymbol{q}_e \\ & - \frac{k_v + \hat{c}(t)\Theta + \Delta_{max}\xi\|\boldsymbol{D}\|\|\boldsymbol{v}_1\|}{1-\Delta_{max}\xi\|\boldsymbol{D}\|}\tilde{\boldsymbol{\omega}}_a\Bigg). \quad (40)\end{aligned}$$

Now, we shall state the following theorem:

Theorem 1 *Consider the attitude tracking error system in* (4) *and* (8) *under assumptions 1-5. Suppose that the control parameters k_v, α_2, and σ are chosen to satisfy the condition* (30)*. If the inertia-free adaptive continuous commanded control input $\boldsymbol{u}_c$ is given by* (40) *and the update law is provided by* (22)*, then the sliding vector $\tilde{\boldsymbol{\omega}}$, attitude tracking error $\boldsymbol{q}_e$, and angular velocity tracking error $\boldsymbol{\omega}_e$ are uniformly ultimately bounded, and converge to a small invariant set containing the origin, that is, $\lim_{t\to\infty}\|\tilde{\boldsymbol{\omega}}(t)\| \in \Omega_{\tilde{\boldsymbol{\omega}}}$, $\lim_{t\to\infty}\boldsymbol{q}_e(t) \in \Omega_{\boldsymbol{q}_e}$, and $\lim_{t\to\infty}\boldsymbol{\omega}_e(t) \in \Omega_{\boldsymbol{\omega}_e}$, where $\Omega_{\tilde{\boldsymbol{\omega}}}$, $\Omega_{\boldsymbol{q}_e}$, and $\Omega_{\boldsymbol{\omega}_e}$ are defined as $\Omega_{\tilde{\boldsymbol{\omega}}} = \left\{\tilde{\boldsymbol{\omega}}\ \middle|\ \|\tilde{\boldsymbol{\omega}}\| \leq \min\left\{\sqrt{\frac{\eta}{k_1}}, \sigma\right\}\right\}$, $\Omega_{\boldsymbol{q}_e} = \left\{\boldsymbol{q}_e\ \middle|\ \|\boldsymbol{q}_e\| \leq \sqrt{\frac{\eta}{k(k_1 k + k_2)}}\right\}$, $\Omega_{\boldsymbol{\omega}_e} = \left\{\boldsymbol{\omega}_e\ \middle|\ \|\boldsymbol{\omega}_e\| \leq \sqrt{\frac{\eta}{k_1}}\right\}$, respectively.*

Proof. In *Case I*, if the condition (30) is satisfied, then $\dot{V}_s < 0$, and thus $\|\tilde{\boldsymbol{\omega}}\| \leq \epsilon \leq \sigma$ can always be achieved in finite time. In *Case II*, from (34), it can be shown that the closed-loop systems is uniformly ultimately bounded stable [34]. Summarizing *Case I* and *Case II*, it can be concluded that all the internal signals are bounded. Furthermore, if the condition (30) and equation (36)

are satisfied, it follows that $\dot{V}_s < 0$ for both *Case I* and *Case II*. As a result, the overall closed-loop system is bounded and the decrease of $\dot{V}_s$ drives $\|\tilde{\boldsymbol{\omega}}\|$ and $\|\boldsymbol{q}_e\|$ into $\|\tilde{\boldsymbol{\omega}}\| \leq \min\left\{\sqrt{\frac{\phi}{k_1}}, \sigma\right\}$ and $\|\boldsymbol{q}_e\| \leq \sqrt{\frac{\phi}{k_2 k}}$ ultimately. Moreover, if equation (39) is satisfied, it follows that $\dot{V}_{s1} < 0$ for *Case II*, and thus $\|\boldsymbol{\omega}_e\|$ and $\|\boldsymbol{q}_e\|$ converge to $\|\boldsymbol{\omega}_e\| \leq \sqrt{\frac{\phi}{k_1}}$ and $\|\boldsymbol{q}_e\| \leq \sqrt{\frac{\phi}{k(k_1 k+k_2)}}$ ultimately. Since $\sqrt{\frac{\phi}{k(k_1 k+k_2)}} < \sqrt{\frac{\phi}{k_1}}$, $\|\boldsymbol{q}_e\|$ shall be confined to $\|\boldsymbol{q}_e\| \leq \sqrt{\frac{\phi}{k(k_1 k+k_2)}}$ ultimately. Therefore, it is obtained that the filtered angular velocity, attitude orientation and angular velocity tracking errors are uniformly ultimately bounded as $\lim_{t\to\infty} \|\tilde{\boldsymbol{\omega}}(t)\| \in \Omega_{\tilde{\boldsymbol{\omega}}}$, $\lim_{t\to\infty} \boldsymbol{q}_e(t) \in \Omega_{\boldsymbol{q}_e}$, and $\lim_{t\to\infty} \boldsymbol{\omega}_e(t) \in \Omega_{\boldsymbol{\omega}_e}$, where $\Omega_{\tilde{\boldsymbol{\omega}}}$, $\Omega_{\boldsymbol{q}_e}$, and $\Omega_{\boldsymbol{\omega}_e}$ are small invariant sets containing the origin defined in theorem 2. This completes the proof. □

Remark 3. The stability condition on the control parameters k_v, α_2, and σ in (30) can be relaxed if some modifications are made to the update law (22). The modified update law is proposed as

$$\dot{\hat{c}}(t) = \alpha_1 \Theta \tilde{\boldsymbol{\omega}}_a^T \boldsymbol{D}_\epsilon[\tilde{\boldsymbol{\omega}}] - \frac{\alpha_1}{\Theta}\alpha_2^2(t)\hat{c}(t). \tag{41}$$

This modified update law is employed with an auxiliary time-varying gain function $\alpha_2(t)$ satisfying

$$\dot{\alpha}_2(t) = -\frac{k_\alpha}{\Theta}\alpha_2(t) \tag{42}$$

where k_α is a positive constant.

To show the stability of the closed-loop system under the virtual control input (18) and modified adaptive law (41), the candidate Lyapunov function is chosen as $V_s = \frac{1}{2}\tilde{\boldsymbol{\omega}}^T \boldsymbol{J}\tilde{\boldsymbol{\omega}} + k_2\left[\boldsymbol{q}_e^T\boldsymbol{q}_e + (1-q_{e0})^2\right] + \frac{1}{2\alpha_1}\tilde{c}^2(t) + \frac{1}{8k_\alpha}c^2\alpha_2^2(t)$. Differentiating V_s with respect to time and substituting the virtual control input and modified update law into it, $\dot{V}_s \leq -k_1\|\tilde{\boldsymbol{\omega}}\|^2 - k_2 k\|\boldsymbol{q}_e\|^2 < 0$ can also be obtained in *Case I* without restrictions on the control parameters. This modification on the adaptive law shall not affect the result in *Case II* except that the constant η in (35) becomes $\eta = \frac{\Delta_{max}\xi\|D\|}{1-\Delta_{max}\xi\|D\|}\left(k_v + c_m + k_2 + k_1\sigma\right)\sigma + c\sigma$. Therefore, it is proved similarly that the results stated in theorem 1 can also be achieved. □

Remark 4. From parameter update law in (22), the constant α_1 mainly adjusts the increasing rate of the parameter $\hat{c}(t)$ (the rising phase of $\hat{c}(t)$ if the initial value $\hat{c}(0)$ is small), while α_2 adjusts the decreasing rate (the steady phase of $\hat{c}(t)$). In order to ensure a smooth change of the $\hat{c}(t)$, α_1 and α_2 should be small constants. Moreover, due to the stability condition in (30), a large value of α_2 should not be select. □

4 Simulations

To study the effectiveness and performance of the CA-based FTC strategies, numerical simulations have been carried out for spacecraft attitude tracking system given in (1) under actuator faults/failures. The spacecraft is assumed to have the inertia matrix of $\boldsymbol{J} = [20\ 1.2\ 0.9;\ 1.2\ 17\ 1.4;\ 0.9\ 1.4\ 15]$ kg $\cdot$ m^2. External disturbances are $\boldsymbol{d} = 5\times10^{-2}\,[\sin(0.8t)\ \cos(0.5t)\ \sin(0.2t)]^T$ N $\cdot$ m. In order to achieve three axes control of a spacecraft, four reaction wheels (RW) in a pyramid configuration are considered as actuators, whose distribution matrix is $\boldsymbol{D} = \frac{1}{\sqrt{3}}[-1\ -1\ 1\ 1;\ 1\ -1\ -1\ 1;\ 1\ 1\ 1\ 1]$. For a clear interpretation of the results, attitude are expressed in Euler angles (yaw, pitch, and roll are ψ, θ, and ϕ) converted from unit quaternion in the simulation. The initial attitude is set as $[\psi,\ \theta,\ \phi]^T = [38.85,\ 22.33,\ -16.32]^T$ deg, corresponding to $\boldsymbol{Q}(0) = [-0.2,\ 0.15,\ 0.35,\ 0.9028]^T$. The initial angular velocity is $\boldsymbol{\omega}(0) = [0,\ 0,\ 0]^T$ rad/s. The desired motion expressed in the body frame $\mathcal{B}$ with respect to inertial frame $\mathcal{I}$ is $\boldsymbol{\omega}_d(t) = 0.01[\cos(t/40),\ \sin(t/60),\ -\cos(t/50)]^T$ rad/s. Using $\dot{\boldsymbol{q}}_d = \frac{1}{2}(\boldsymbol{S}(\boldsymbol{q}_d) + q_{d0}\boldsymbol{I}_3)\boldsymbol{\omega}_d$ and $\dot{q}_{d0} = -\frac{1}{2}\boldsymbol{q}_d^T\boldsymbol{\omega}_d$, the desired quaternion $\boldsymbol{Q}_d$ can be obtained, and then the desired attitude represented by Euler angers (ψ_d, θ_d, and ϕ_d) can also be obtained. The initial value of desired quaternion is set as $\boldsymbol{Q}_d(0) = [0,\ 0,\ 0,\ 1]^T$.

In the simulation, four reaction wheels are assume to experience partial loss of effectiveness fault or total failure simultaneously. The detailed scenario is described as

$$\begin{cases} e_1(t) = 0.5 + 0.09\sin(0.05t) + 0.005\,\mathrm{rand}(\cdot) \\ e_2(t) = 0.6 + 0.1\cos(0.08t) + 0.008\,\mathrm{rand}(\cdot) \\ e_3(t) = 0.4 + 0.08\sin(0.06t) + 0.005\,\mathrm{rand}(\cdot) \\ e_4(t) = 0 \end{cases}$$

where the function rand$(\cdot)$ generates a random value from the normal distribution with mean 0 and standard deviation 1. Under this fault scenario, it is found that $\xi = 1.732$ in (12). Here it is assumed that the upper bound on the error in fault estimation is $\Delta_{max} = 0.25$. The parameters of the inertia-free adaptive continuous virtual control input in (18) is set as $k = 0.3$, $k_1 = 0.1$, $k_2 = 0.1$, $\alpha_1 = 0.01$, $\alpha_2 = 0.01$, $\sigma = 0.001$, and $k_v = 0.1$. The initial value of $\hat{c}(t)$ in (22) is chosen as $\hat{c}(0) = 0.01$.

The simulation results using inertial-free adaptive FTC design (18) under the actuator faults/failures are given in Fig. 2. It can be seen that all signals are bounded and tracking errors converge to a small neighborhood of zero despite external disturbances and actuator faults/failures. In particular, it is observed from Figs. 2c that no commanded control input is reallocated to RW4 and the virtual control input is totally reallocated to RW1-RW3. This observation is in accordance with the CA scheme in (9). Referring to Fig. 2d, the adaptive parameter is bounded, and thus the efficacy of the proposed adaptation law is verified.

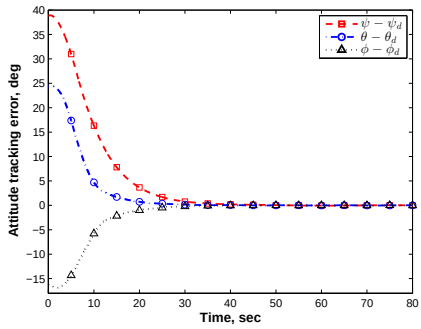

(a) Attitude orientation tracking error.

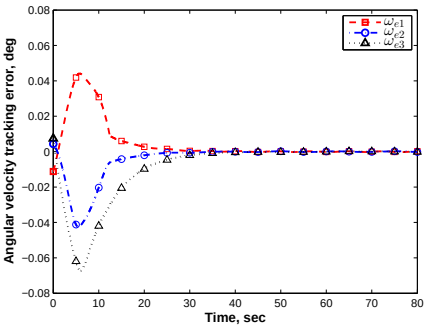

(b) Angular velocity tracking error.

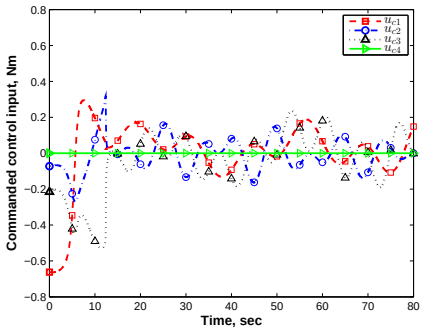

(c) Commanded control input.

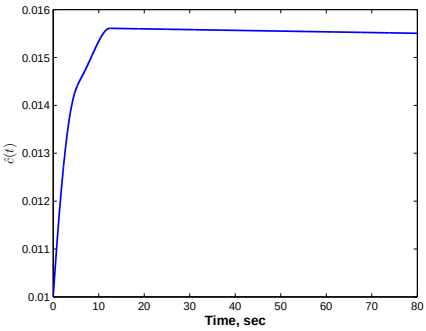

(d) Adaptive parameter $\hat{c}(t)$.

Fig. 2. Tracking errors, commanded control input $\boldsymbol{u}_c$, and adaptive parameter using inertia-free adaptive FTC law in (18).

Table 1
Comparison of control performance

Controller	Control performance		
	SE[1] of $\boldsymbol{q}_e$	SE of $\boldsymbol{\omega}_e$	OCF[2]
Proposed FTC law in (40)	$\pm$ 0.06	$\pm$ 3×10^{-4}	5.93
FTC law in [17]	$\pm$ 1.15	$\pm$ 5×10^{-3}	10.56
PD+ controller [35] with CA in [15]	$\pm$ 6.50	$\pm$ 2×10^{-2}	3.13

[1] SE stands for steady error.
[2] OCF denotes overall control effort defined as OCF $= \frac{1}{2}\int_0^T \|\boldsymbol{u}_c\| dt$, where T is the simulation time.

For the purposes of comparison, the FTC attitude tracking controller in [17] and the PD+ controller in [35] combined with CA in [15] are also simulated under the same fault scenario. The control gains of PD+ controller are turned such that the closed-loop attitude tracking error system in healthy condition is critical damping. To make a fair comparison of the control performances under actuator faults/failures, the magnitude of control torques under three control schemes are limited to the same level. The comparison results are summarized in Table 1. It is observed that the proposed FTC law in (40) provides superior control performance than the two controller schemes used for comparison. Since there is no fault recovery in PD+ controller, it doesn't cost extra control effort to compensate for actuator faults and the tracking performance has deteriorated significantly. From energy consumption perspective, the proposed FTC law uses less control effort and achieves better control performance comparing with FTC law in [17].

5 Conclusions

In this paper, a CA-based FTC scheme for attitude tracking systems of over-actuated spacecraft in the presence of actuator faults/failures and external disturbances are presented. Due to the availability of actuator redundancies, CA is used to redistribute the control efforts among remaining actuators without reconfiguring the controller, and faulty but not completely failed actuators are fully leveraged. A novel adaptive FTC scheme is proposed without using the information on the inertia matrix and external disturbances. It is shown that the proposed FTC scheme has the capacity to handle actuator faults/failures and the uniform ultimate boundedness of the tracking errors can be ensured. The effectiveness of the proposed FTC schemes is verified through simulation of a rigid spacecraft. In future work, control input saturation and unwinding problem should be investigated to reduce the power consumption.

Appendix

A Proof of Lemma 1

From (21), $\|\tilde{\boldsymbol{\omega}}_a\| = 1$ when $\|\tilde{\boldsymbol{\omega}}\| > \epsilon$ which implies that $\tilde{\boldsymbol{\omega}}^T\tilde{\boldsymbol{\omega}}_a = \tilde{\boldsymbol{\omega}}^T\frac{\tilde{\boldsymbol{\omega}}}{\|\tilde{\boldsymbol{\omega}}\|} = \|\tilde{\boldsymbol{\omega}}\|$ for $\|\tilde{\boldsymbol{\omega}}\| > \epsilon$. If $\|\tilde{\boldsymbol{\omega}}\| \leq \epsilon$, then $\|\tilde{\boldsymbol{\omega}}_a\| = \frac{\|\tilde{\boldsymbol{\omega}}\|}{\epsilon} \leq 1$ and $\tilde{\boldsymbol{\omega}}^T\tilde{\boldsymbol{\omega}}_a = \frac{\|\tilde{\boldsymbol{\omega}}\|^2}{\epsilon} \leq \epsilon$. Notice that $\epsilon = \frac{\sigma}{\Theta}$ and $\Theta \geq 1$, it follows that $\tilde{\boldsymbol{\omega}}^T\tilde{\boldsymbol{\omega}}_a \leq \sigma$ for $\|\tilde{\boldsymbol{\omega}}\| \leq \epsilon$. Therefore, the results in lemma 1 are established. □

B Proof of Lemma 2

When $\|\tilde{\boldsymbol{\omega}}\| \leq \epsilon$, it is clear that $\|\tilde{\boldsymbol{\omega}}\| \leq \frac{\sigma}{\Theta}$. Since $\|\tilde{\boldsymbol{\omega}}\| = \|\boldsymbol{\omega} - \bar{\boldsymbol{\omega}}_d\|$ from (7), it follows that $\|\tilde{\boldsymbol{\omega}}\| \geq \|\boldsymbol{\omega}\| - \|\bar{\boldsymbol{\omega}}_d\|$. This gives $\Theta \leq \frac{\sigma}{\Theta} + c_\omega + k + 1$, where the inequality in (13) is used. Since $\Theta = \|\omega\| + 1 \geq 1$, it can be obtained that $\Theta^2 - (c_\omega + k + 1)\,\Theta - \sigma \leq 0$. Consequently, solving this inequality yields $1 \leq \Theta \leq \Theta_m$, where $\Theta_m = \frac{c_\omega + k + 1 + \sqrt{(c_\omega + k + 1)^2 + 4\sigma}}{2}$. $\square$

References

[1] Z. Chen and J. Huang. Attitude tracking and disturbance rejection of rigid spacecraft by adaptive control. *IEEE Transactions on Automatic Control*, 54(3):600–605, 2009.

[2] W. Luo, Y. Chu, and K. Ling. Inverse optimal adaptive control for attitude tracking of spacecraft. *IEEE Transactions on Automatic Control*, 50(11):1639–1654, 2005.

[3] J. D. Boskovic, S. Li, and R. K. Mehra. Robust tracking control design for spacecraft under control input saturation. *Journal of Guidance, Control, and Dynamics*, 27(4):627–633, 2004.

[4] K. Lu and Y. Xia. Adaptive attitude tracking control for rigid spacecraft with finite-time convergence. *Automatica*, 19(12):3591–3599, Dec. 2014.

[5] C. G. Mayhew, R. G. Sanfelice, and A. R. Teel. Quaternion-based hybrid control for robust global attitude tracking. *IEEE Transactions on Automatic Control*, 56(11):2555–2566, Nov. 2011.

[6] A. Tayebi. Unit quaternion-based output feedback for the attitude tracking problem. *IEEE Transactions on Automatic Control*, 53(6):1516–1520, Jul. 2008.

[7] G. Tao, S. M. Joshi, and X. Ma. Adaptive state feedback and tracking control of systems with actuator failures. *IEEE Transactions on Automatic Control*, 46(1):78–95, Jan. 2001.

[8] B. Robertson and E. Stoneking. Satellite GN&C anomaly trends. In *AAS Guidance and Control Conference*, AAS 03-071, 2003.

[9] M. Blanke, M. Kinnaert, J. Lunze, and M. Staroswiecki. *Diagnosis and Fault-Tolerant Control*. Springer, Berlin, Germany, 2 edition, 2006.

[10] Y. Zhang and J. Jiang. Bibliographical review on reconfigurable fault-tolerant control systems. *Annual Reviews in Control*, 32(2):229–252, Dec. 2008.

[11] J. Jiang and X. Yu. Fault-tolerant control systems: A comparative study between active and passive approaches. *Annual Reviews in Control*, 36(1):60–72, Apr. 2012.

[12] Y. Shtessel, J. Buffington, and S. Banda. Tailless aircraft flight control using multiple time scale reconfigurable sliding modes. *IEEE Transactions on Control Systems Technology*, 10(2):288–296, 2002.

[13] M. L. Corradini, G. Orlando, and G. Parlangeli. A fault tolerant sliding mode controller for accommodating actuator failures. In *Proc. 44th IEEE Conf. Decision and Control*, pages 3091–3096, 2005.

[14] Y. W. Liang and S. D. Xu. Reliable control of nonlinear systems via variable structure scheme. *IEEE Transactions on Automatic Control*, 51(10):1721–1726, Oct. 2006.

[15] H. Alwi and C. Edwards. Fault tolerant control using sliding modes with on-line control allocation. *Automatica*, 44(7):1859–1866, Jul. 2008.

[16] J. D. Boskovic, S. Li, and R. K. Mehra. Intelligent control of spacecraft in the presence of actuator failures. In *Proc. 38th IEEE Conf. Decision and Control*, volume 5, pages 4472–4477, Phoenix, AZ, 1999.

[17] W. Cai, X. Liao, and Y. Song. Indirect robust adaptive fault-tolerant control for attitude tracking of spacecraft. *Journal of Guidance, Control, and Dynamics*, 31(5):1456–1463, 2008.

[18] J. Jin, S. Ko, and C. K. Ryoo. Fault tolerant control for satellites with four reaction wheels. *Control Engineering Practice*, 16(10):1250–1258, Oct. 2008.

[19] Y. W. Liang, S. D. Xu, and C. L. Tsai. Study of VSC reliable designs with application to spacecraft attitude stabilization. *IEEE Transactions on Control Systems Technology*, 15(2):332–338, Mar. 2007.

[20] B. Xiao, Q. Hu, D. Wang, and E. K. Poh. Attitude tracking control of rigid spacecraft with actuator misalignment and fault. *IEEE Transactions on Control Systems Technology*, 21(6):2360 – 2366, Nov. 2013.

[21] O. Harkegard and T. Glad. Resolving actuator redundancy-optimal control vs. control allocation. *Automatica*, 41(1):137–144, 2005.

[22] J. Burken, P. Lu, Z. Wu, and C. Bahm. Two reconfigurable flight-control design methods: Robust servomechanism and control allocation. *Journal of Guidance, Control, and Dynamics*, 24(3):482–493, May-Jun. 2001.

[23] J. Tjønnås and T. A. Johansen. Adaptive control allocation. *Automatica*, 44(11):2754–2765, Nov. 2008.

[24] M. T. Hamayun, C. Edwards, and H. Alwi. Design and analysis of an integral sliding mode fault-tolerant control scheme. *IEEE Transactions on Automatic Control*, 57(7):1783–1789, Jul. 2012.

[25] M. T. Hamayun, C. Edwards, and H. Alwi. A fault tolerant control allocation scheme with output integral sliding modes. *Automatica*, 49(6):1830–1837, Jun. 2013.

[26] D. Verbin and V. J. Lappas. Rapid rotational maneuvering of rigid satellites with hybrid actuators configuration. *Journal of Guidance, Control, and Dynamics*, 36(2):532–547, Mar.-Apr. 2013.

[27] V. T. Ahmed, J. Coppola and D. Bernstein. Adaptive asymptotic tracking of spacecraft attitude motion with inertia matrix identification. *Journal of Guidance, Control, and Dynamics*, 21(5):684–691, Sep.-Oct. 1998.

[28] B. T. Costic, D. M. Dawson, M. S. Queiroz, and V. Kapila. Quaternion-based adaptive attitude tracking controller without velocity measurements. *Journal of Guidance, Control, and Dynamics*, 24(6):1214–1222, 2001.

[29] D. Thakur, S. Srikant, and M. R. Akella. Adaptive attitude-tracking control of spacecraft with uncertain time-varying inertia parameters. *Journal of Guidance, Control, and Dynamics*, 38(1):41–52, Jan. 2015.

[30] P. C. Hughes. *Spacecraft attitude dynamics*. Mineola, N.Y. : Dover Publications, 2004.

[31] J. J. E. Slotine and W. Li. On the adaptive control of robot manipulators. *The International Journal of Robotics Research*, 6(3):49–59, 1987.

[32] R. Kristiansen, P. J. Nicklasson, and J. T. Gravdahl. Spacecraft coordination control in 6DOF: Integrator backstepping vs passivity-based control. *Automatica*, 44(11):2896–2901, November 2008.

[33] G. W. Stewart. On scaled projections and pseudoinverses. *Linear Algebra and its Applications*, 112:189–193, 1989.

[34] H. K. Khalil. *Nonlinear Systems*. Prentice-Hall, Upper Saddle, River, NJ, 3rd edition, 2002.

[35] J. T. Wen and K. Kreutz-Delgado. The attitude control problem. *IEEE Transactions on Automatic Control*, 36(10):1148–1162, Oct. 1991.